# Experimental Comparison of Manufacturing Parameters in Automotive Friction Materials

Furkan Akbulut[1]* (iD), İbrahim Mutlu[2] (iD)

[1.]*Department of Motor Vehicles and Transportation Tech., Technical Sciences Vocational School, Hitit University, Çorum, 19030, Turkey*
[2.]*Automotive Engineering Department, Faculty of Technology, Afyon Kocatepe University, Afyonkarahisar, 03010, Turkey*

**Research Article**

## Abstract

In this study, a fixed automotive friction material content was determined and the mechanical and tribological effects of manufacturing parameters on friction materials were investigated. Parameters; pre-forming time (1-3-5 min) and pre-forming pressure (8-10-12 MPa), hot pressing time (5-10-15 min) hot pressing pressure (8-10-12 MPa) and hot pressing temperature (125-150-175 °C), curing time (4-8-12 h) and curing temperature (120-150-180 °C) were determined. The friction test of the produced samples was carried out under 0.551 MPa pressure and 7 m/s rotation speed for 90 min. In addition, the average COF, friction stability, specific wear rate, density and hardness values of the samples were calculated. According to the results obtained, the average COF value increased as the pre-forming time and pressure increased. The lowest specific wear rate among all specimens was calculated as $7.622 \times 10^{-6}$ $cm^3$/Nm in PFP-12 specimen. With the increase in hot pressing time, the tribological properties of friction materials improved. The highest friction stability among all samples was calculated as 79.42% in the HPT-15 sample. Although there was an increase in the average COF value with increasing hot pressing pressure and temperature, the specific wear rates increased in these parameters. The highest average COF value among all samples was obtained in the CT-12 sample with a value of 0.553. The specific wear rate increased with the increase in curing time and temperature. The highest specific wear rate among all samples was calculated $10,743 \times 10^{-6}$ $cm^3$/Nm in the CTe-180 sample. Finally, it has been suggested that 3 min for pre-forming time, 12 MPa for pre-forming pressure; 15 min for hot pressing time, 12 MPa for hot pressing pressure, and 150°C for hot pressing temperature; and a curing time of 8 h and curing temperature of 150 °C may be sufficient.

*Keywords*: Friction materials; Manufacturing parameters; Optimization; Wear

## 1. Introduction

The brake system is one of the most basic safety systems of a vehicle [1–3]. Friction occurs during braking, which causes active wear of the friction and disc surfaces of the friction materials [4]. This is where friction materials come into play. Friction materials are an important component of the braking system in vehicles. It is the friction material that attaches to the brake system and comes into contact with the brake disc or rotor when the brakes are applied. This friction produces the force necessary to slow or stop the vehicle. Over the past 110 years, innovations in modern friction materials have played a significant role in improving the overall performance of automotive braking systems [5–8]. These innovations have led to advances in friction materials, including the development of new composite materials that provide better braking efficiency, less wear and better thermal conductivity. In the past, asbestos-based friction materials were commonly used in friction materials due to their high coefficient of friction and durability. However, asbestos has been banned in many countries due to the health hazards it poses. The composition of friction materials consists of various components, including binders, fibers, fillers, friction materials, lubricants and abrasives [9–16]. The correct selection and composition of these components is crucial in determining the friction behavior, wear resistance and thermal performance of friction materials. Friction materials are designed to withstand high temperatures and repeated friction forces without significant wear or degradation [17,18].

In the manufacturing sector, achieving optimum performance and efficiency is crucial to ensuring high quality products. One of the areas where optimization plays an important role is the production of friction materials. Optimization of manufacturing parameters in friction materials is of great importance as it directly affects the performance and safety of the brake system.

By carefully controlling and adjusting various factors such as molding pressure, temperature, time and heat treatment, manufacturers can improve the tribological properties of friction materials, ultimately contributing to the improvement of brake performance, durability and overall safety. Manufacturing optimization allows the production of friction materials that meet industry standards for performance and safety. It helps reduce manufacturing costs by determining the most efficient and cost-effective parameters and processes. The optimization ensures a consistent and stable friction level throughout the life of the friction materials, minimizing vibrations, noise and wear on both the rotor and friction material. Moreover, optimization of manufacturing parameters is of great importance to meet increasingly stringent requirements and expectations for friction materials. Optimization of manufacturing parameters in friction materials is a complex and critical process. It requires an in-depth understanding of the tribological properties of friction materials as well as the various factors that can affect their performance [19,20].

The manufacturing parameters of automotive friction materials are critical to braking performance and safety. Many of these parameters are determined by the resin manufacturer. This is because the thermal properties, which are affected by the high temperatures generated during braking, directly influence the manufacturing conditions. In particular, the molecular structure of the resin directly affects the fading behavior observed during braking. Thermal degradation of the resin at high temperatures leads to a weakening of the friction materials. This causes the friction force and braking efficiency to drop to unacceptably low levels. This jeopardizes braking safety. Therefore, resin formulation and production parameters must be optimized to improve friction stability at high temperatures. The resin should be modified to show minimal dependence on temperature and the manufacturing parameters should be selected within optimal limits [21–24].

Ertan and Yavuz (2010) did an experiment on a friction material composition to find out how different manufacturing parameters affect tribological properties and to find the best manufacturing parameters for better tribological behavior. The results showed that the manufacturing parameters can significantly improve the tribological behavior and production cost of the brake pad, as long as the optimum values are selected [24]. Wilairat et al. (2019) examined the effects of hot molding conditions on the porosity and compressibility of friction materials. The results and correlation coefficients showed that molding pressure and molding time had the most significant effects on porosity and compressibility [25]. Aleksendric and Senatore (2012) investigated how brake friction material wear was impacted by the manufacturing parameters. In their investigation, they employed a hybrid (neuro-genetic) optimization model. For common brake interface temperatures, it was discovered how the most significant manufacturing parameters; molding pressure, molding temperature, molding time, heat treatment temperature, and heat treatment time, affect the wear of various friction material types (different formulations and production conditions). It has been shown that the wear of some types of friction materials is significantly affected by their manufacturing parameter [26].

In this study, the effect of manufacturing parameters on automotive friction material was investigated experimentally. A fixed content was determined, pre-forming time and pressure; hot pressing time, pressure and temperature; curing time and temperature were optimized.

## 2. Material Method

A fixed content has been determined in the manufacturing of automotive friction material. Table 1 shows the materials and their ratios used in the production of friction material. Binder, phenolic resin; metal content, bronze powder and brass shavings; fiber, glass fiber and steel wool; filler material, barite; lubricant graphite and friction modifier $Al_2O_3$ were used. Since the aim of the study was to optimize the manufacturing parameters, the most known materials in the literature were preferred for friction material manufacturing. The materials used in the study were selected through a comprehensive literature review. It is the most widely used phenolic resin for friction materials. Phenolic resin has good mechanical properties and is inexpensive. It is also more resistant to solvents, acids and water than other resins. Barites are heavy-density, inert minerals. They are inexpensive because they can be mined anywhere in the world. Since it does not easily change its properties at temperatures exceeding 300 °C, it is resistant to high temperatures. A naturally occurring type of crystalline carbon is graphite. Because it does not easily react with other elements, it is often used in the production of different lubricants. Its lubricating properties are great. minimizes the noise of the brakes [27–37].

Table 1. Fixed content used in the production of friction material

| Classification | Materials | Contents (%) |
|---|---|---|
| Binder | Phenolic Resin | 15 |
| Metal Content | Bronze | 5 |
|  | Brass Shaving | 5 |
| Fiber | Glass Fiber | 15 |
|  | Steel Wool | 5 |
| Filler | Barite | 40 |
| Lubricant | Graphite | 5 |
| Friction Modifier | $Al_2O_3$ | 10 |

Samples were produced using the powder metallurgy method, one of the conventional fabrication techniques. Powder materials were calculated in the determined volumes and added to the mixing device and the mixing process was carried out. Mixing is the first step in friction material production. This process depends on various factors such as the order of adding the ingredients, mixing time and speed. Each parameter affects the quality

of the mixture, which defines the microstructure and properties of the friction material [38,39]. Under good mixing conditions, mixing times of 10 to 15 min are sufficient to ensure a well-mixed mixture [39]. The mixing phase was implemented in two steps in order to mix the powder materials to be used in production homogeneously. First, it was mixed in a V-shaped mixing device for 30 min at a rotation speed of 15 rpm. Then, it was mixed in a rondo mixer at a rotation speed of 1200 rpm for 1 min. In order to obtain the material without dispersing during the pre-forming stage, the prepared powder mixtures were sprayed with 3% alcoholic water on the mixture before being put into the mold. After the mixing process, samples were produced by applying pre-forming, hot pressing and curing steps. The detailed flow chart of the manufacturing process of the samples, the devices used in the manufacturing process and the visuals of the samples are shown in Figure 1.
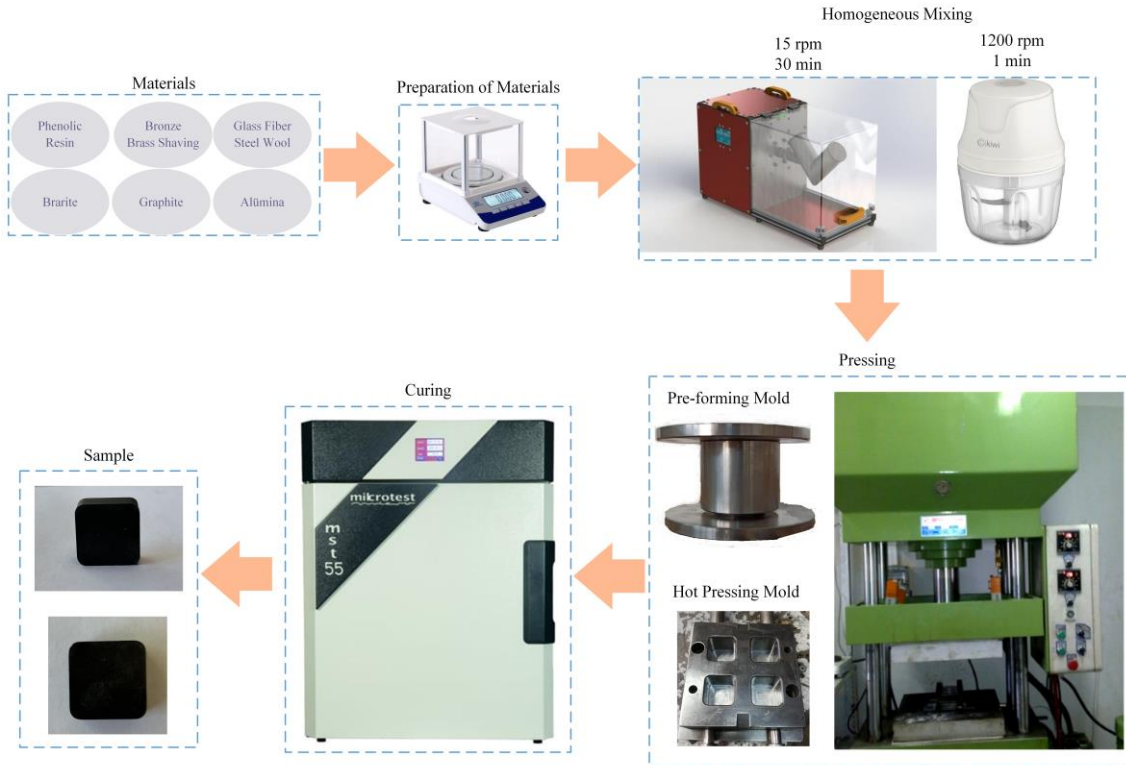


Fig. 1. Flowchart of the manufacturing process of the samples

In manufacturing parameter optimization; pre-forming pressing time and pressure, hot pressing time-pressure and temperature, curing time and temperature parameters were determined. The experimental parameters specified in this study were determined according to the parameters commonly used in the literature [40–45] and the capacities of the devices at the manufacturing process. Manufacturing parameter values are given in Table 2. When Table 2 is examined, 1, 3 and 5 min for pre-forming pressing time, 8, 10 and 12 MPa for pre-forming pressing pressure; 5, 10 and 15 min for hot pressing time, 8, 10 and 12 MPa for hot pressing pressure, 125, 150 and 175 °C for hot pressing temperature; curing time values of 4, 8 and 12 h and curing temperature values of 120, 150 and 180 °C were determined. In manufacturing optimization, one of the parameter values was changed and the others were kept constant, thus the effect of all parameters was recorded. Friction-wear tests of the produced samples were carried out on the friction wear test device shown in Figure 2.

Table 2. Experimental plan for manufacturing parameters optimization

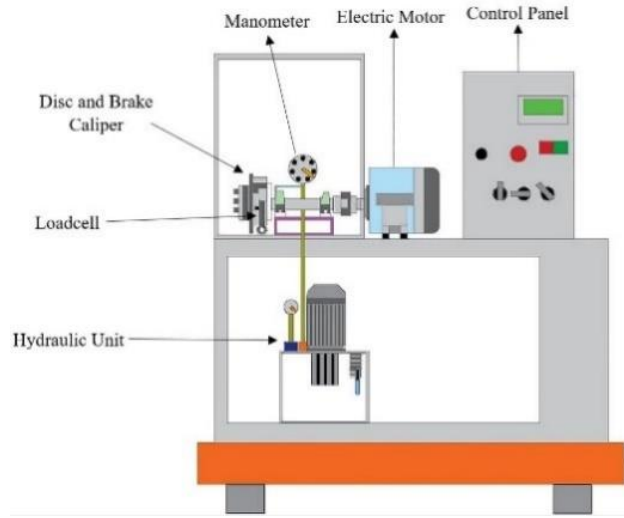| Parameter | Code | Value | | |
|---|---|---|---|---|
| Pre-Forming Time (min) | PFT | 1 | 3 | 5 |
| Pre-Forming Pressure (MPa) | PFP | 8 | 10 | 12 |
| Hot Pressing Time (min) | HPT | 5 | 10 | 15 |
| Hot Pressing Pressure (MPa) | HPP | 8 | 10 | 12 |
| Hot Pressing Temperature (°C) | HPTe | 125 | 150 | 175 |
| Curing Time (h) | CT | 4 | 8 | 12 |
| Curing Temperature (°C) | CTe | 120 | 150 | 180 |

Fig. 2. Schematic view of friction wear tester

The friction coefficient-temperature change of the samples was determined by the FAST (Friction Assessment and Screening Test) method by measuring every second for 5400 s under 0.551 MPa pressure and 7 m/s speed.

Density values of friction materials were determined according to Archimedes' principle. Density measurements were carried out in an experimental setup operating according to the Archimedes principle. The formula used for density measurement is shown in Eq. (1). Three different density values were taken for each sample and the density of each sample was determined by taking the average of these values.

$$\rho_s = \frac{m_a}{m_a - m_w} \rho_w \tag{1}$$

Where, $\rho_s$ is the density of sample, $m_a$ is the mass of the sample in air, $m_w$ is the mass of the sample in water, $\rho_w$ is the density of water.

Hardness measurements of the samples were carried out with the Shore D durometer hardness measuring device. Measurements were determined according to the ASTM D2240 standard by measuring from 3 different points of the material and calculating the averages.

The specific wear rate was calculated according to the mass loss method as specified in TS 555. Before starting the wear tests, the masses of the samples were weighed and recorded using a precision balance with an accuracy of 0.001 g. Likewise, their masses were weighed and recorded after the experiment. This was determined as mass loss. The specific wear rate used for the calculation is shown in Eq. (2).

$$V = \frac{1}{2\pi R_d} \frac{m_1 - m_2}{n f_m \rho} \tag{2}$$

Where V is the specific wear rate (cm$^3$/Nm), $m_1$ is the mass measured before the experiment, $m_2$ is the mass measured after

the experiment, $\rho$ is the sample density, $R_d$ is the disc radius, $f_m$ is the average friction force, n is the number of revolutions.

Friction stability is determined as a function of braking pressure and sliding speed. The magnitude of friction stability should be as high as possible and close to 100. In addition, the slope and fluctuations in the friction curve should be minimal. Friction stability is determined by the ratio of the average friction coefficient to the maximum friction coefficient and is expressed as a percentage. The calculation of friction stability is shown in Eq. (3).

$$FS = \frac{\mu_{ave}}{\mu_{max}} \tag{3}$$

Where $\mu_{ave}$ is the average friction coefficient obtained during the experiment, $\mu_{max}$ is the maximum friction coefficient obtained during the experiment.

The surface roughness of some samples after the experiment was measured using a three-dimensional optical profilometer. In accordance with the ISO25178 standard, surface roughness values were recorded. These values include the Root Mean Square Height (Sq), the Maximum Peak Height (Sp), the Maximum Pit Height (Sv), Maximum Height (Sz) and the average surface roughness (Sa). Measurements were carried out on the wearing surface of the samples in an area of 100x100 µm$^2$, with a scanning step interval of 5 µm and a scanning frequency of 2000 Hz.

## 3. Results and Discussions

The experiments were carried out with pre-forming times of 1, 3 and 5 min and the results were recorded. Figure 3,4,5 and 6 shows the average COF, time-dependent COF-temperature curve, friction stability-specific wear rate, density and hardness results of the samples produced by varying the pre-forming time, respectively.
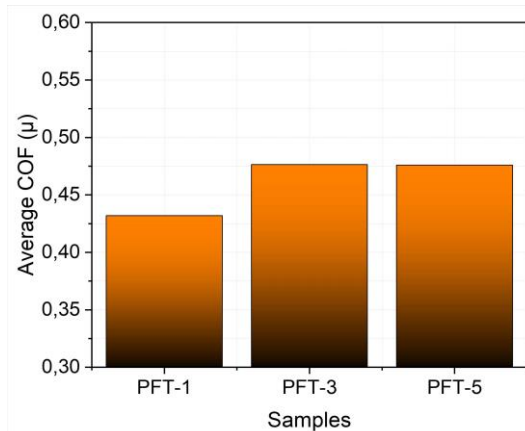


Fig. 3. Results of PFT-1, PFT-3 and PTF-5 samples average COF

When Figure 3 is examined, the highest average COF value was obtained in PFT-3 specimen which was pre-formed for 3

min with 0.476. The lowest average COF value was obtained in the PFT-1 specimen, which was pre-formed for 1 min with 0.431. It was observed that the average COF values of PFT-3 and PFT-5 samples were very close to each other.
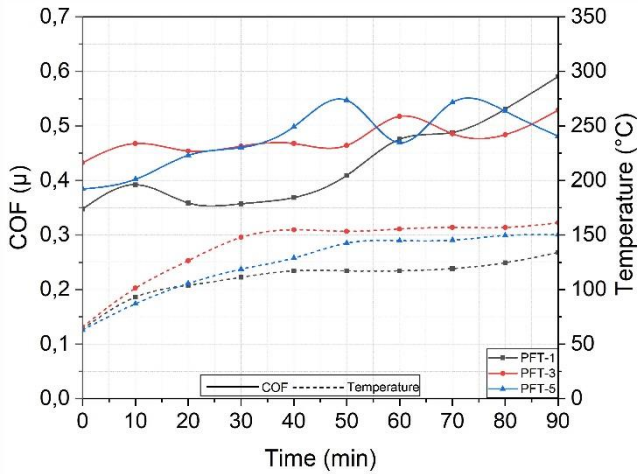


Fig. 4. Results of PFT-1, PFT-3 and PTF-5 samples time-dependent COF-temperature curve

When the time-dependent COF-temperature curve is analyzed in Figure 4, it is seen that the PFT-3 sample draws a more stable friction curve than the other samples. In parallel with this, in Figure 5, the friction stability was higher than the other two samples and was calculated as 79.01%. As the pre-forming time increased, the specific wear value decreased and the specific wear values of PFT-3 and PFT-5 samples were close to each other. The highest specific wear rate was calculated in PFT-1 sample.
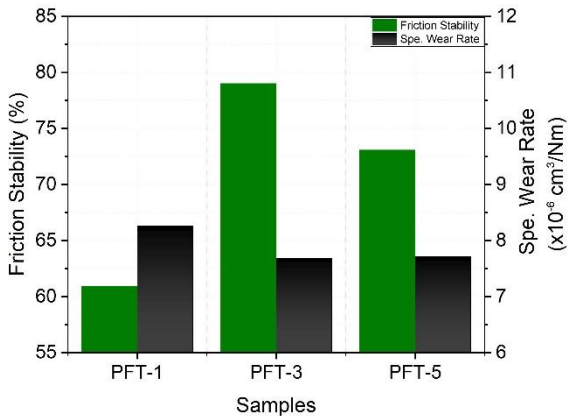


Fig. 5. Results of PFT-1, PFT-3 and PTF-5 samples friction stability-specific wear rate

The lowest hardness value was seen in the PFT-1 sample. Density values were close to each other for the 3 samples. The average density value of PFT-1, PFT-3 and PFT-5 samples was calculated as 2.732 g/cm$^3$ and the hardness value was calculated as 89.89 Shore D. It was determined that 1 min pre-forming time was insufficient as it exhibited lower average COF and friction stability and higher specific wear value compared to PFT-3 and PFT-5 samples.
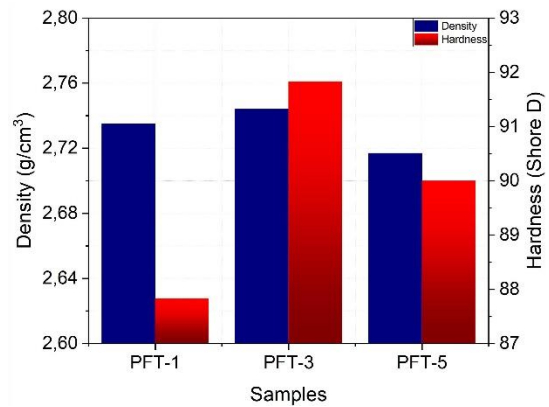


Fig. 6. Results of PFT-1, PFT-3 and PTF-5 samples density and hardness

Experiments for pre-forming pressure were carried out with 8, 10 and 12 MPa pre-forming pressures and the results were recorded. Figures 7,8,9 and 10 show the average COF, time-dependent COF-temperature curve, friction stability-specific wear rate, density and hardness results of the samples produced by varying the pre-forming pressure, respectively. In figure 7 were examined, it was observed that the results of the PFP-8 and PFP-10 samples were very close to each other, and the average COF value of the PFP-12 sample was higher than the other samples. The average COF value of the PFP-12 sample was determined to be 0.50.
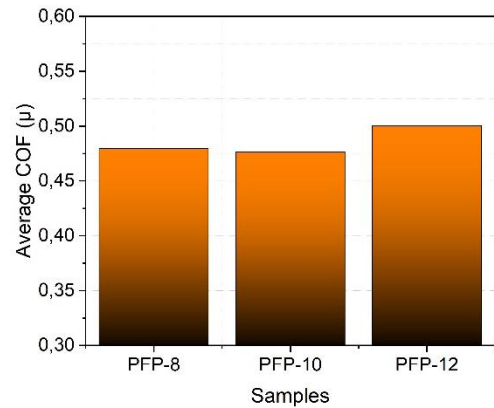


Fig. 7. Results of PFP-8, PFP-10 and PFP-12 samples average COF

When Figure 8 is examined, the PFP-10 sample had a more stable friction curve, the other samples showed an increase in the general curve until the 80th min, and then there was a decrease in the curve. The lowest friction stability and the highest specific wear value were observed in the PFP-8 sample.
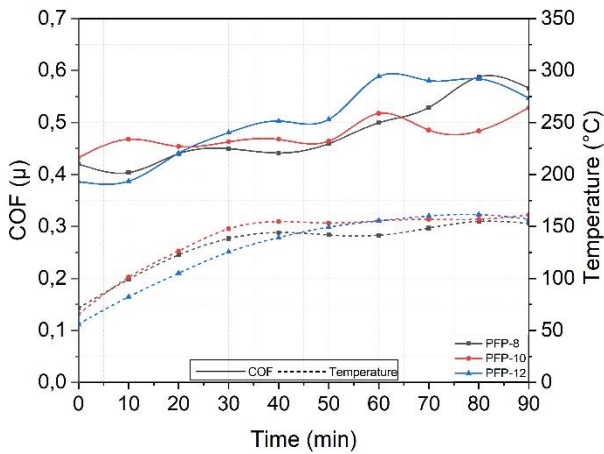
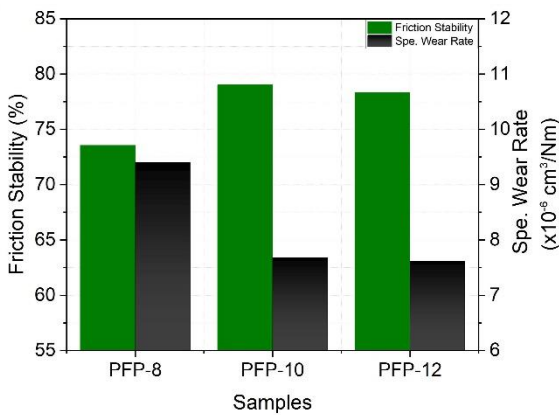Fig. 8. Results of PFP-8, PFP-10 and PFP-12 samples time-dependent COF-temperature curve



Fig. 9. Results of PFP-8, PFP-10 and PFP-12 samples friction stability-specific wear rate

In Figure 9, it is seen that the friction stabilities and specific wear values of the PFP-10 and PFP-12 samples are close to each other. It was observed that the specific wear rate decreased with increasing pre-forming pressure. The lowest specific wear rate was obtained in the PFP-12 sample.
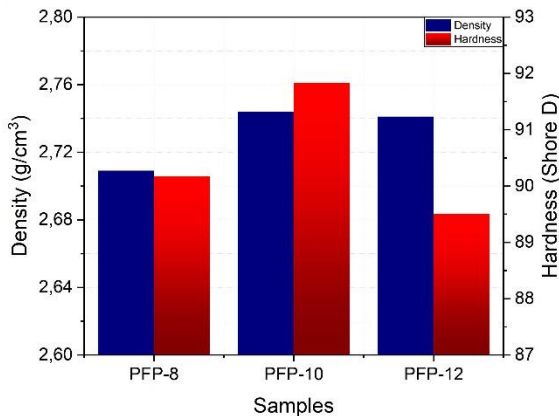


Fig. 10. Results of PFP-8, PFP-10 and PFP-12 samples density and hardness

In figure 10, the lowest density value is obtained in the PFP-8 sample, and the density values of the PFP-10 and PFP-12 samples are close to each other. The highest hardness value was seen in the PFP-10 sample. The average density values for PFP-8, PFP-10 and PFP-12 samples were calculated as 2.731 g/cm$^3$ and hardness values as 90.5 Shore D.

For hot pressing time, samples were produced by pressing for 5, 10 and 15 min. Figures 11,12,13 and 14 show the average COF, time-dependent COF-temperature curve, friction stability-specific wear rate, density and hardness values of the samples produced by varying the hot pressing time, respectively.
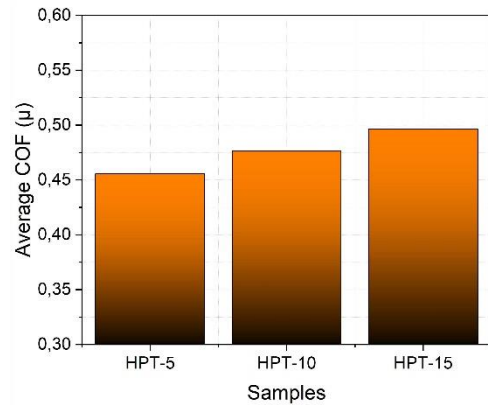


Fig. 11. Results of HPT-5, HPT-10 and HPT-15 samples average COF

In Figure 11 and 13 are examined that it was observed that the average COF value and friction stability increased as the hot pressing time increased. The highest average COF value among the hot pressing times was obtained in the HPT-15 sample pressed for 15 min with a value of 0.496. Similarly, when Figure 13 is examined, it was determined that the friction stability increased as the hot pressing time increased and the highest friction stability was observed in the HPT-15 sample with 79.42%. The lower average COF and stability as the hot pressing time decreases, the higher specific wear rate value, can be explained by the fact that bonding times for powder materials are insufficient, resulting in poor bonding between powders. Since insufficient bonding occurred, the highest specific wear rate and the lowest average COF and stability values were seen in the HPT-5 sample pressed for 5 min. The friction stabilities of the HPT-10 and HPT-15 samples were very close to each other. Similarly, the specific wear rate showed a decreasing trend as the hot pressing time increased, and the specific wear values of the HPT-10 and HPT-15 samples were very close to each other. When the time-dependent COF-temperature curves are examined in Figure 12, it is observed that the coefficient of friction of the HPT-15 sample has an increasing trend until the 30th min, and then a more stable coefficient of friction curve is observed until the end of the experiment compared to the other samples. When Figure 14 is analyzed that the highest density and hardness values were obtained in the HPT-10 sample. The average density value of HPT-5, HPT-10 and HPT-15 samples was calculated as 2.713 g/cm$^3$ and the hardness value was 89.72 Shore D.
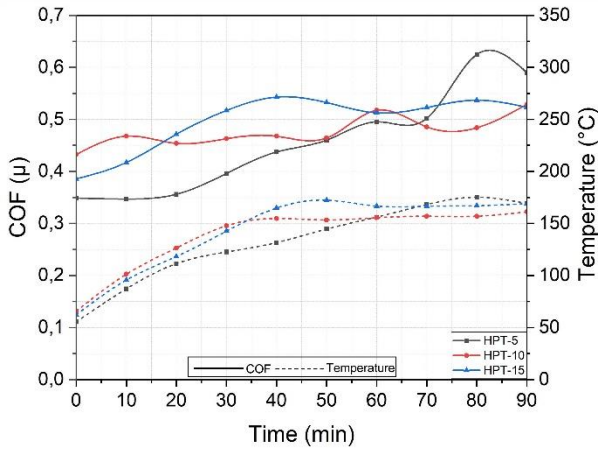
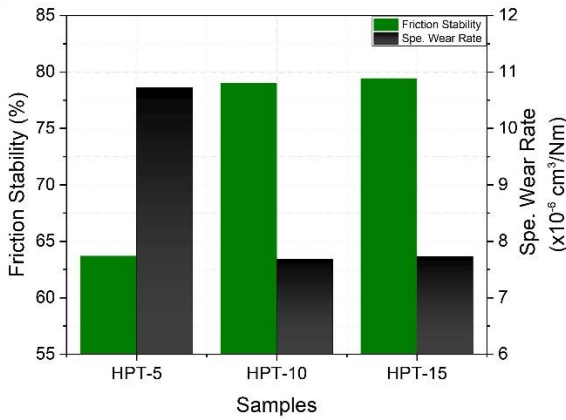Fig. 12. Results of HPT-5, HPT-10 and HPT-15 samples time-dependent COF-temperature curve



Fig. 13. Results of HPT-5, HPT-10 and HPT-15 samples friction stability-specific wear rate
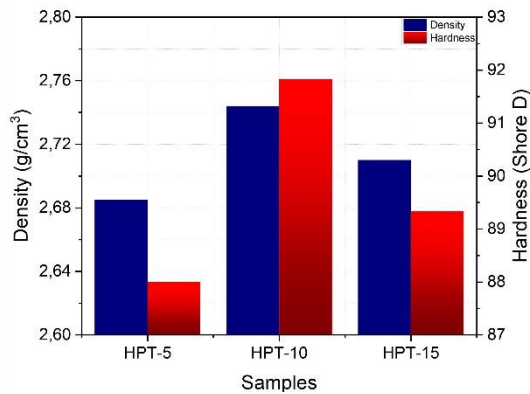


Fig. 14. Results of HPT-5, HPT-10 and HPT-15 samples density and hardness

For hot pressing pressure, experiments were carried out with 8, 10 and 12 MPa pressing pressures and the results were recorded. Figures 15,16,17 and 18 show the average COF, time-dependent COF-temperature curve, friction stability-specific wear rate, density and hardness results of the samples produced by changing the hot pressing pressures, respectively.
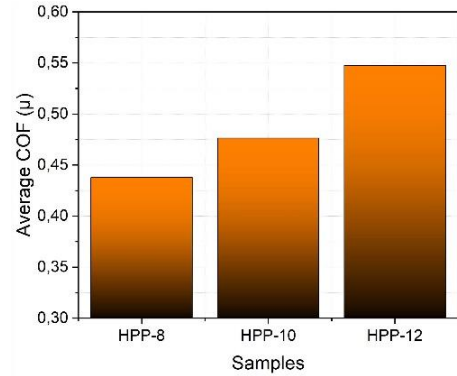


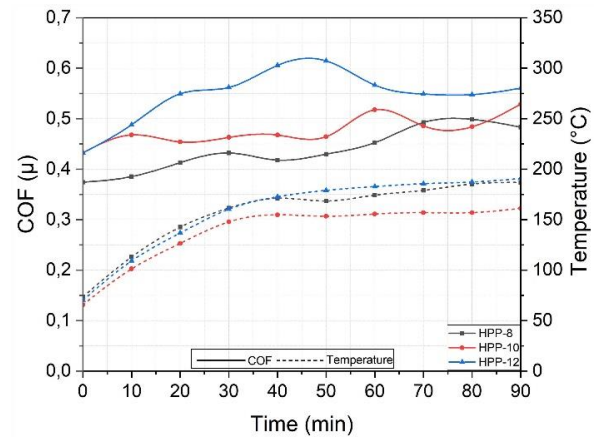Fig. 15. Results of HPP-8, HPP-10 and HPP-12 samples average COF



Fig. 16. Results of HPP-8, HPP-10 and HPP-12 samples time-dependent COF-temperature curve

When Figure 15 is examined The average COF values of HPP-8, HPP-10 and HPP-12 samples increased with increasing pressing pressure. The highest average COF value was obtained in HPP-12 sample with 0.547. In Figure 17, Although the HPP-12 sample had the highest average COF value, the HPP-10 sample had the highest friction stability and the lowest specific wear rate. Figure 16 shows that HPP-8, HPP-10 and HPP-12 samples generally follow a stable friction curve, especially HPP-12 sample shows a very stable curve after 60 min.
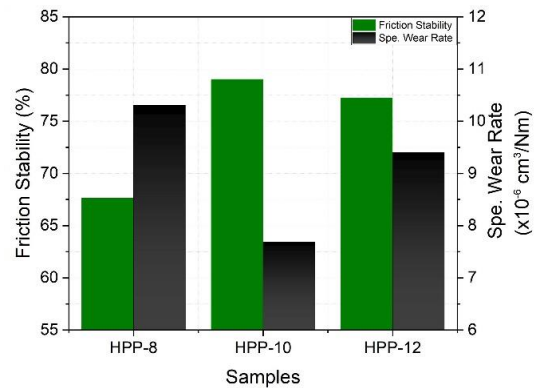


Fig. 17. Results of HPP-8, HPP-10 and HPP-12 samples friction stability-specific wear rate
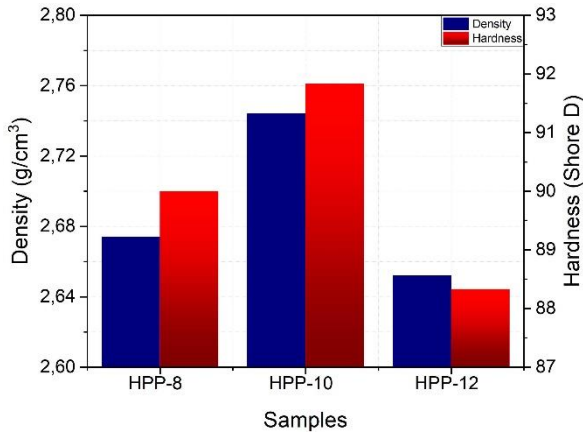
Fig. 18. Results of HPP-8, HPP-10 and HPP-12 samples density and hardness

The highest density and hardness values were obtained in the HPP-10 sample. The average density value of HPP-8, HPP-10 and HPP-12 samples was calculated as 2.69 g/cm$^3$ and the hardness value was calculated as 90.05 Shore D.

Samples were produced by varying the hot pressing temperature as 125, 150 and 175 °C and the results were recorded. Figure 19,20,21 and 22 show the average COF, time-dependent COF-temperature curve, friction stability-specific wear rate, density and hard-ness results of the samples produced by changing the hot pressing pressures, respectively.
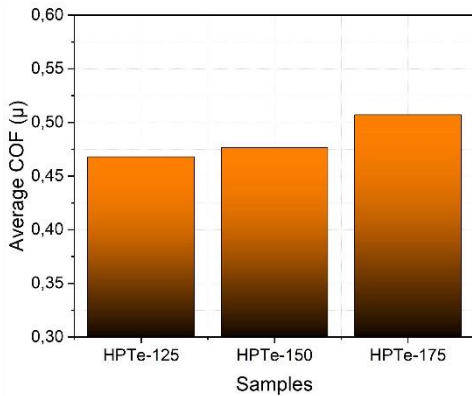


Fig. 19. Results of HPTe-125, HPTe-150 and HPTe-175 samples average COF

When Figure 19 is examined, it is seen that the average COF value increases as the hot pressing time increases, and the highest average COF value of 0.507 was obtained in the HPTe-175 sample pressed at 175 °C.

The time-dependent COF-temperature curve shows that the HPTe-175 sample has an increasing COF curve until the end of the experiment. HPTe-125 and HPTe-150 samples show a more stable COF curve. The highest frictional stability and the lowest wear rate were obtained in the HPTe-150 sample. The highest density and hardness values were obtained in the HPTe-150 sample. The average density value of HPTe-125, HPTe-150 and

HPTe-175 samples was calculated as 2.719 g/cm$^3$ and the hardness value was calculated as 90.72 Shore D.
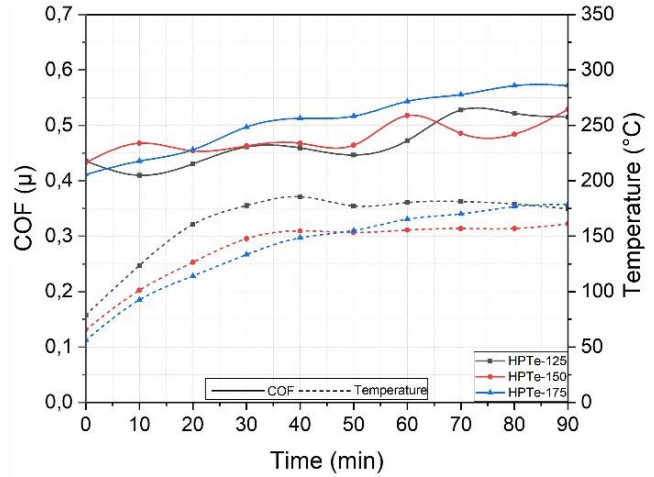


Fig. 20. Results of HPTe-125, HPTe-150 and HPTe-175 samples time-dependent COF-temperature curve
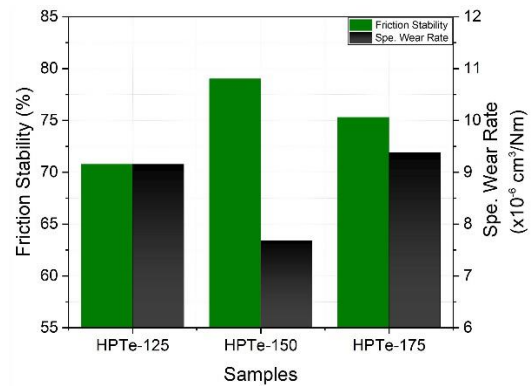


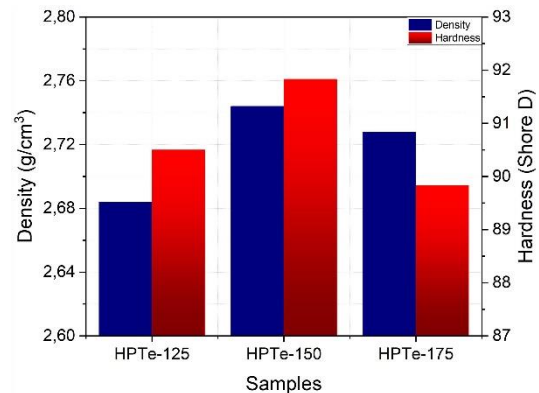Fig. 21. Results of HPTe-125, HPTe-150 and HPTe-175 samples friction stability-specific wear rate



Fig. 22. Results of HPTe-125, HPTe-150 and HPTe-175 samples density and hardness

After the hot pressing process, the samples were produced by keeping them in a drying oven for 4, 8 and 12 h to investigate the effect of curing time. Figures 23,24,25 and 26 show the average COF, time-dependent COF-temperature curve, friction

stability-specific wear rate, density and hardness results of the samples produced by changing the hot pressing pressures, respectively.
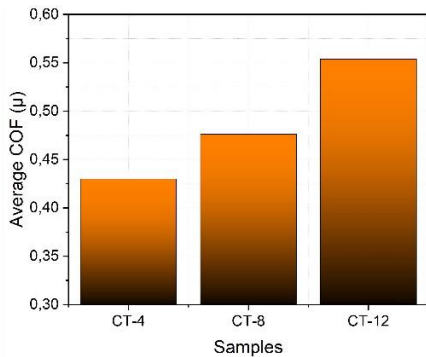


Fig. 23. Results of CT-4, CT-8 and CT-12 samples average COF

As the curing time increased, the average COF values of the samples increased. The highest friction stability and lowest specific wear rate occurred in the CT-8 sample cured for 8 h. When the friction curve is examined, it is seen that the CT-12 sample exhibits an increase in the friction curve throughout the experiment. The highest density and hardness values were seen in the CT-8 sample. The average density value of CT-4, CT-8 and CT-12 samples was calculated as 2.713 g/cm$^3$ and the hardness value was 91.17 Shore D.



Fig. 24. Results of CT-4, CT-8 and CT-12 samples time-dependent COF-temperature curve



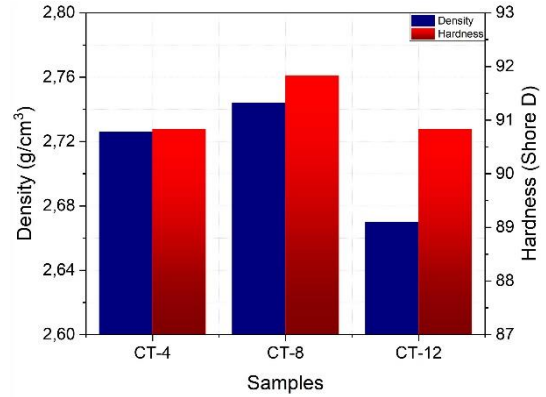Fig. 25. Results of CT-4, CT-8 and CT-12 samples friction stability-specific wear rate



Fig. 26. Results of CT-4, CT-8 and CT-12 samples density and hardness

Samples were produced by varying the curing temperature as 120, 150 and 180 °C and the results were recorded. Figure 27,28,29 and 30 show the average COF, time-dependent COF-temperature curve, friction stability-specific wear rate, density and hardness results of the samples produced by changing the hot pressing pressures, respectively.
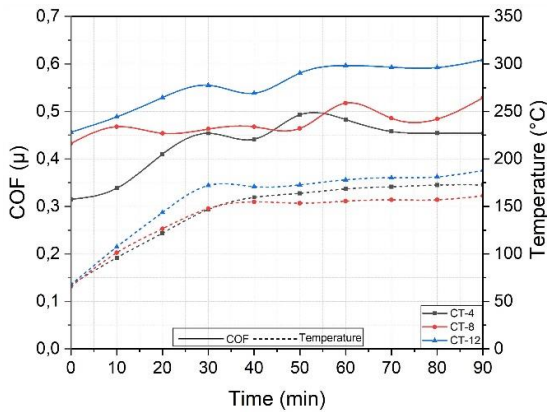


Fig. 27. Results of CTe-120, CTe-150 and CTe-180 samples average COF



Fig. 28. Results of CTe-120, CTe-150 and CTe-180 samples time-dependent COF-temperature curve
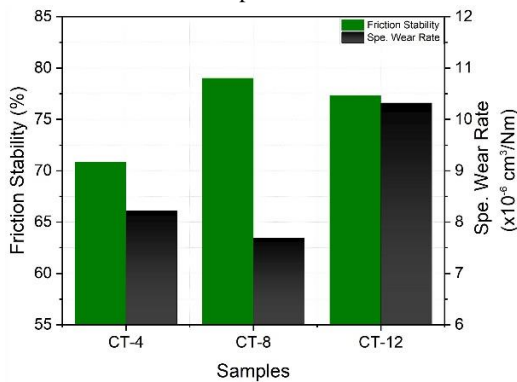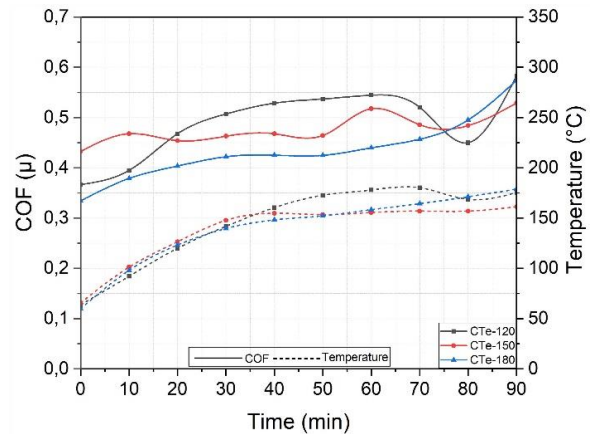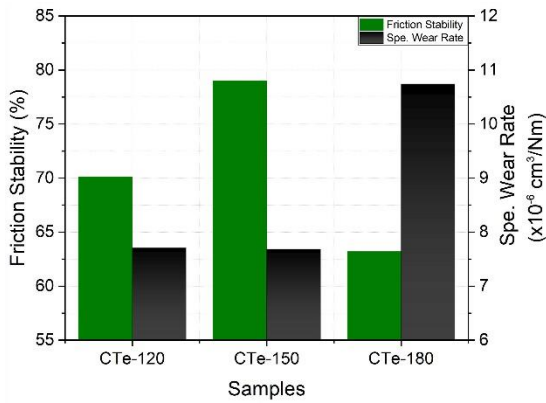
Fig. 29. Results of CTe-120, CTe-150 and CTe-180 samples friction stability-specific wear rate
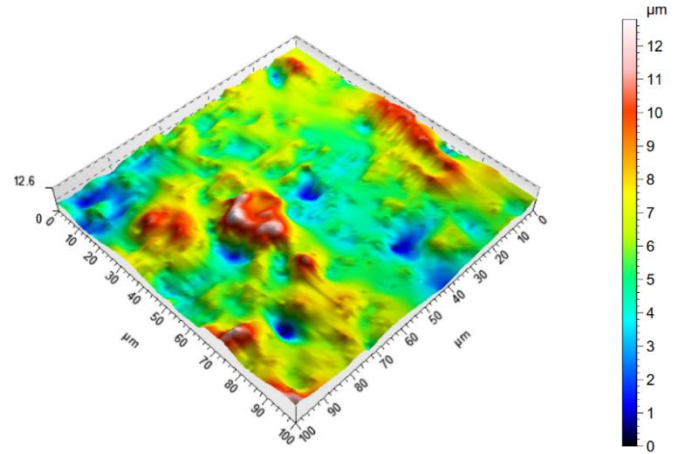


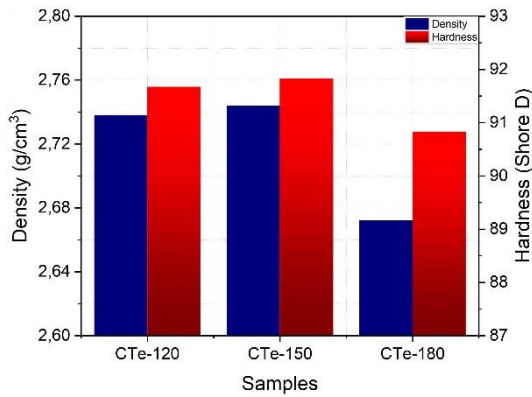Fig. 31. 3D profilometer image of PFP-12 sample



Fig. 30. Results of CTe-120, CTe-150 and CTe-180 samples density and hardness
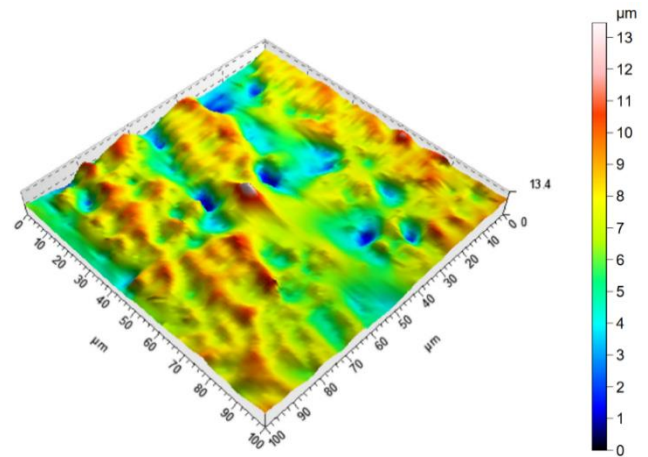


Fig. 32. 3D profilometer image of HPT-15 sample

When the results are examined, the average COF value decreases as the curing temperature increases. The lowest friction stability and highest specific wear rate were obtained in the CTe-180 sample cured at 180 °C. It has been stated that above a certain heat treatment temperature, the structure of the friction material deteriorates and the material's resistance to fading decreases [24]. The highest density and hardness values were seen in the CTe-150 sample. The average density value of CTe-120, CTe-150 and CTe-180 samples was calculated as 2.718 g/cm$^3$ and the hardness value was 91.44 Shore D.

Figure 31 shows the 3D profilometer result of the PFP-12 sample. According to the results, Sq, Sp, Sv, Sz and Sa values were measured as 1.75, 6.71, 6.09, 12.08 and 1.33 respectively. Figure 32 shows the 3D profilometer result of the HPT-15 sample. According to the results, Sq, Sp, Sv, Sz and Sa values were measured as 1.65, 6.49, 6.37, 13.5 and 1.32 respectively. The density of PFP-12 and HPT-15 samples was measured as 2.741 and 2.71, respectively. It was observed that Sz and Sv values increased as the density decreased. Less dense friction material can be more easily fragmented and crumbled during wear. It is thought that this fragmentation and crumbling may cause the formation of pits and heights on the friction material surface.

## 4. Conclusions

The conclusions obtained as a result of the experimental studies are listed below.

* As the pre-forming time increased, the average COF value of the samples generally increased. When the pre-forming time was applied for 5 min, although the average COF of the sample was almost the same, friction stability, density and hardness values decreased, and the specific wear rate increased. Increasing the pre-forming pressure increased the average COF value of the samples and decreased the specific wear rate value.

* Among the pre-forming parameters, 3 min of pressing time and 12 MPa pressing pressure were found sufficient.

* Increasing the hot pressing time helped to improve the tribological properties of the friction material. With increasing hot pressing time, the average COF value increased by 9%, friction stability increased by 24% and specific wear rate decreased by 28%. However, at 10 and 15 min pressing times, friction stability and specific wear rate values were not affected much and showed values close to each other.

* With the increase of hot pressing pressure, the average COF value increased by 25%. However, the lowest specific wear rate was calculated in the HPP-10 sample pressed at 10 MPa pressure.

* Similar to hot pressing pressure, the average COF value increased by 8% with the increase of hot pressing temperature. However, the lowest specific wear rate was calculated in the HPTe-150 sample.

* Among the hot pressing parameters, it was found sufficient that the pressing time was 15 min, the pressing pressure was 12 MPa and the pressing temperature was 150 °C.

* The highest COF was obtained in the sample cured for 12 h. However, the specific wear value of this sample was much higher than the others.

* With the increase in curing temperature, the average COF values of the samples decreased. The average COF values of the samples decreased with increasing curing temperature. As the curing temperature increased from 120 °C to 180 °C, the average COF value of the friction material decreased by 12% and the specific wear rate increased by 38%.

* Among the curing parameters, a curing time of 8 h and a curing temperature of 150 °C were found sufficient.

## Acknowledgment

## Nomenclature

| | |
|---|---|
| *PFT* | : pre-forming time (min) |
| *PFP* | : pre-forming pressure (MPa) |
| *HPT* | : hot pressing time (min) |
| *HPP* | : hot pressing pressure (MPa) |
| *HPTe* | : hot pressing temperature |
| *CT* | : curing time (h) |
| *CTe* | : curing temperature (°C) |
| *V* | : specific wear rate ($cm^3$/Nm) |
| *COF* | : coefficient of friction (μ) |
| *FAST* | : Friction Assessment and Screening Test |

## Conflict of Interest Statement

The authors declare that there is no conflict of interest in the study.

## CRediT Author Statement

**Furkan Akbulut**: Investigation, Methodology, Writing-original draft, **İbrahim Mutlu**: Conceptualization, Supervision,

## References

[1] Akbulut F, Mutlu İ. The Effect of Sintering Time on the Tribological Properties of Automotive Brake Pads. Int J Automot Eng Technol. 2023;12(1) :16-21. https://doi.org/10.18245/ijaet.1223599.

[2] Sugözü İ, Sugözü B. Investigation of Usage of Milled Pine Cone in Brake Pads. Int J Automot Sci Technol. 2020;4(4): 253 - 257 https://doi.org/10.30939/ijastech..770050

[3] Güney B, Mutlu I. Tribological Properties of Brake Discs Coated with Cr2O3-40% TiO2 by Plasma Spraying. Surf Rev Lett. 2019;26(10) https://doi.org/10.1142/S0218625X19500756.

[4] Güney B, Öz A. Microstructure and Chemical Analysis of Vehicle Brake Wear Particle Emissions. Eur J Sci Technol. 2020;19: 633-642 https://doi.org/10.31590/ejosat.744098

[5] Achebe CH, Obika EN, Chukwuneke JL, Ani OE. Optimisation of Hybridised Cane Wood–Palm Fruit Fibre Frictional Material. Proc Inst Mech Eng Part L J Mater Des Appl. 2019;233(12):2490-2497. https://doi.org/10.1177/1464420719863445.

[6] Karaman M, Korucu SA. Modeling the vehicle movement and braking effect of the hydrostatic regenerative braking system. Engineering Perspective. 2023;3(2). https://doi.org/10.5505/pajes.2013.55264

[7] Akincıoğlu G, Akincıoğlu S, Öktem H, Uygur İ. Brake Pad Performance Characteristic Assessment Methods. Int J Automot Sci Technol. 2021;5(1):67-78. https://doi.org/10.30939/ijastech..848266.

[8] Yavuz H, Bayrakçeken H. Investigation of Friction and Wear Behavior of Composite Brake Pads Produced with Huntite Mineral. Int J Automot Sci Technol. 2022;6(1):9-16. https://doi.org/10.30939/ijastech..1022247.

[9] Yavuz H, Bayrakçeken H. Friction and Wear Response of Automobile Brake Pad Composites Containing Volcanic Tuff. J Aust Ceram Soc. 2023;59(5):1465-1476. https://doi.org/10.1007/s41779-023-00952-1.

[10] Sugözü B, Sugözü İ. Investigation of the Use of a New Binder Material in Automotive Brake Pad. Int J Automot Sci Technol. 2020;4(4):258-263. https://doi.org/10.30939/ijastech..772922.

[11] Akıncıoğlu G. Evaluation of the Effect of the Novolac Resin Ratio on the High-Temperature Performance of the Brake Pads. Int J Automot Sci Technol. 2022;6(2):196-201. https://doi.org/10.30939/ijastech..1087420.

[12] Akbulut F, Kılıç H, Mutlu İ, Öztürk FS, Çaşın E, Seyrek M, vd. Investigation of Tribological Properties of Brake Friction Materials Developed from Industrial Waste Products. Int J Automot Sci Technol. 2023;7(4):309–315. https://doi.org/10.30939/ijastech..1373026.

[13] Hendre KN, Bachchhav BD. Friction and Wear Characteristics of Rubber Resin-Bonded Metallic Brake Pad Materials. Int J Eng Adv Technol. 2019;8(6):1312-1316. 10.35940/ijeat.F8514.088619.

[14] Akıncıoğlu G, Akıncıoğlu S, Öktem H, Uygur İ. Wear Response of Non-Asbestos Brake Pad Composites Reinforced with Walnut Shell Dust. J Aust Ceram Soc. 2020;56(3) https://doi.org/10.1007/s41779-020-00452-6.

[15] Akıncıoğlu G, Uygur İ, Akıncıoğlu S, Öktem H. Friction-wear Performance in Environmentally Friendly Brake Composites: A Comparison of Two Different Test Methods. Polym Compos. 2021;42(9) https://doi.org/10.1002/pc.26162.

[16] Singh T. Comparative Performance of Barium Sulphate and Cement by-pass Dust on Tribological Properties of Automotive Brake Friction Composites. Alexandria Eng J. 2023;72: 339-349. https://doi.org/10.1016/j.aej.2023.04.010

[17] Ma Y, Shen S, Tong J, Ye W, Yang Y, Zhou J. Effects of Bamboo Fibers on Friction Performance of Friction Materials. J

Thermoplast Compos Mater. 2013;26(6):845-859 https://doi.org/10.1177/0892705712461513.

[18] Öktem H, Akıncıoğlu S, Uygur İ, Akıncıoğlu G. A Novel Study of Hybrid Brake Pad Composites: New Formulation, Tribological Behaviour and Characterisation of Microstructure. Plast Rubber Compos. 2021;50(5):249-261.
https://doi.org/10.1080/14658011.2021.1898881

[19] Shinde D, Mistry KN. Asbestos base and Asbestos Free Brake Lining Materials: Comparative Study. Int J Sci World. 2017;5(1):192-198. https://doi.org/10.14419/ijsw.v5i1.7082.

[20] Sugözü B, Dağhan B, Akdemir A. Effect of the Size on the friction Characteristics of Brake Friction Materials: A Case Study with $Al_2O_3$. Ind Lubr Tribol. 2018;70(6):1020-1024.
https://doi.org/10.1108/ILT-02-2017-0035.

[21] Hong US, Jung SL, Cho KH, Cho MH, Kim SJ, Jang H. Wear Mechanism of Multiphase Friction Materials With Different Phenolic Resin Matrices. Wear. 2009;266(7–8):739-744.
https://doi.org/10.1016/j.wear.2008.08.008

[22] Bijwe J, Nidhi, Majumdar N, Satapathy BK. Influence of Modified Phenolic Resins on the Fade and Recovery Behavior of Friction Materials. Wear. 2005;259(7–12):1068-1078.
https://doi.org/10.1016/j.wear.2005.01.011

[23] EL-Tayeb NSM, Liew KW. On the Dry and Wet Sliding Performance of Potentially New Frictional Brake Pad Materials for Automotive Industry. Wear. 2009;266(1–2):275-287.
https://doi.org/10.1016/j.wear.2008.07.003

[24] Ertan R, Yavuz N. An Experimental Study on the Effects of Manufacturing Parameters on the Tribological Properties of Brake Lining Materials. Wear. 2010;268(11–12):1524–1532.
https://doi.org/10.1016/j.wear.2010.02.026

[25] Wilairat T, Saechin N, Buggakupta W, Sujaridworakun P. Effects of Hot Molding Parameters on Physical and Mechanical Properties of Brake Pads. Key Engineering Materials. 2019;824:59–66.
https://doi.org/10.4028/www.scientific.net/KEM.824.59

[26] Aleksendrić D, Senatore A. Optimization of Manufacturing Process Effects on Brake Friction Material Wear. J Compos Mater. 2012;46(22). 10.1177/0021998311432489

[27] Çengelci E, Bayrakçeken H. Investigation of the Use of Pumice Stone as Automotive Friction Material. J Mater Mechatronics A. 2023;4(1):50-63. https://doi.org/10.55546/jmm.1202932

[28] Ekpruke E, Ossia CV, Big-Alabo A. Recent Progress and Evolution in the Development of Non-Asbestos Based Automotive Brake Pad- A Review. J Manuf Eng. 2022;17(2):51-63.
https://doi.org/10.37255/jme.v17i2pp051-063

[29] Jayashree P, Matějka V, Leonardi M, Straffelini G. The Influence of the Addition of Different Kinds of Slags on the Friction and Emission Behavior of a Commercially Employed Friction Material Formulation. Wear. 2023;522.
https://doi.org/10.1016/j.wear.2023.204705

[30] Menapace C, Leonardi M, Matějka V, Gialanella S, Straffelini G. Dry Sliding Behavior and Friction Layer Formation in Copper-Free Barite Containing Friction Materials. Wear. 2018;398–399:191-200. https://doi.org/10.1016/j.wear.2017.12.008

[31] Venkatesh S, Murugapoopathiraja K. Scoping Review of Brake Friction Material for Automotive. Materials Today: Proceedings. 2019;16(2):927-933. https://doi.org/10.1016/j.matpr.2019.05.178

[32] Nogueira APG, da Silva Gehlen G, Neis PD, Ferreira NF, Gialanella S, Straffelini G. Rice Husk as a Natural Ingredient for Brake Friction Material: A pin-on-disc Investigation. Wear. 2022;494–495. https://doi.org/10.1016/j.wear.2022.204272

[33] Li C, Fu Y, Wang B, Zhang W, Bai Y, Zhang L, vd. Effect of Pore Structure on Mechanical and Tribological Properties of Paper-Based Friction Materials. Tribol Int. 2020;148.
https://doi.org/10.1016/j.triboint.2020.106307

[34] Gehlen GS, Neis PD, Barros LY, Poletto JC, Ferreira NF, Amico SC. Tribological Performance of Eco-Friendly Friction Materials With Rice Husk. Wear. 2022;500–501.
https://doi.org/10.1016/j.wear.2022.204374

[35] Gehlen GS, Nogueira APG, Carlevaris D, Barros LY, Poletto JC, Lasch G, vd. Tribological Assessment of Rice Husk Ash in Eco-Friendly Brake Friction Materials. Wear. 2023;516–517.
https://doi.org/10.1016/j.wear.2022.204613

[36] Tavangar R, Moghadam HA, Khavandi A, Banaeifar S. Comparison of Dry Sliding Behavior and Wear Mechanism of Low Metallic and Copper-Free Brake Pads. Tribol Int. 2020;151.
https://doi.org/10.1016/j.triboint.2020.106416

[37] Österle W, Dmitriev AI. The Role of solid lubricants for Brake Friction Materials. Lubricants. 2016;4(1):5,.
https://doi.org/10.3390/lubricants4010005

[38] Makni F, Cristol AL, Elleuch R, Desplanques Y. Organic Brake Friction Composite Materials: Impact of Mixing Duration on Microstructure, Properties, Tribological Behavior and Wear Resistance. Polymers (Basel). 2022;14(9):1692.
https://doi.org/10.3390/polym14091692

[39] Rupiyawet K, Kaewlob K, Sujaridworakun P, Buggakupta W. Optimization of Mixing Conditions on the Physical and Tribological Properties of Brake Pads. Key Engineering Materials. 2019;824:67-72.

[40] Sugozu I, Mutlu I, Sugozu KB. The Effect of Ulexite to the Tribological Properties of Brake Lining Materials. Polym Compos. 2018;39(1). https://doi.org/10.1002/pc.23901

[41] Sugözü İ, Sugözü B. Friction and Wear Properties of Automobile Brake Linings Containing Borax Powder with Different Grain Sizes. Int J Automot Sci Technol. 2021;5(3):224-227.
https://doi.org/10.30939/ijastech..924897

[42] Mutlu I, Eldogan O, Findik F. Tribological Properties of Some Phenolic Composites Suggested for Automotive Brakes. Tribol Int. 2006;39(4):317-325.
https://doi.org/10.1016/j.triboint.2005.02.002

[43] Lee PW, Filip P. Friction and Wear of Cu-free and Sb-free Environmental Friendly Automotive Brake Materials. Wear. 2013;302(1–2). https://doi.org/10.1016/j.wear.2012.12.046

[44] Yun R, Filip P, Lu Y. Performance and evaluation of Eco-Friendly Brake Friction Materials. Tribol Int. 2010;43(11).
https://doi.org/10.1016/j.triboint.2010.05.001

[45] Mutlu I, Sugözü I, Keskin A. The Effects of porosity in Friction Performance of Brake Pad Using Waste Tire Dust. Polimeros. 2015;25(5). https://doi.org/10.1590/0104-1428.1860